

Unusual Stepwise Assembly and Molecular Growth: $[\text{H}_{14}\text{Mo}_{37}\text{O}_{112}]^{14-}$ and $[\text{H}_3\text{Mo}_{57}\text{V}_6(\text{NO})_6\text{O}_{189}(\text{H}_2\text{O})_{12}(\text{MoO})_6]^{21-}$

Achim Müller,* Jochen Meyer, Erich Krickemeyer, Christian Beugholt, Hartmut Bögge, Frank Peters, Marc Schmidtman, Paul Kögerler, and Michael James Koop

Dedicated to Professor Edgar Niecke on the occasion of his 60th birthday

Abstract: The understanding of the formation of complex molecular systems from simple building blocks by conservative self-assembly processes is still a challenge. We report the synthesis and structural characterization of the large reduced polyoxometallate compounds $(\text{NH}_4)_{14}[\text{H}_{14}\text{Mo}_{37}\text{O}_{112}] \cdot 35 \text{H}_2\text{O}$ (**1**), $(\text{NH}_4)_{21}[\text{H}_3\text{Mo}_{57}\text{V}_6(\text{NO})_6\text{O}_{183}(\text{H}_2\text{O})_{18}] \cdot 55 \text{H}_2\text{O}$ (**2**) (by an improved synthesis) and $\text{Na}_3(\text{NH}_4)_{18}[\text{H}_3\text{Mo}_{63}\text{V}_6(\text{NO})_6\text{O}_{195}(\text{H}_2\text{O})_{12}] \cdot 41 \text{H}_2\text{O}$ (**3**). The cluster systems are formed by a stepwise growth

process. This implies the appearance, during the cluster formation, of ephemeral polyoxometallate intermediates (some of which we were able to isolate). The negative charge and therefore the nucleophilicity of the intermediate cluster fragments increase when they are reduced, resulting in further attraction

of electrophiles and thus in growth of molecular systems. In the case of the cluster anion of **3** we observed, correspondingly, the loss of an $\{\text{MoO}\}^{4+}$ oxometallate fragment by air oxidation; this implies that its uptake and release are controlled by the degree of reduction of the cluster. Correspondingly, intermediates between the anions of **2** and **3** of the $\{\text{Mo}_{57+x}\text{V}_6\}$ type could be isolated. The unusual anion of **1** is formed by symmetry breaking processes.

Keywords: clusters • molecular growth • molybdenum • polyoxometallates • self-assembly

Introduction

Optimally functioning complex molecules or natural products in the biosphere are most elegantly produced stepwise, either under genetic control or epigenetically through self-assembly under dissipative conditions, which means far from equilibrium (natura naturans).^[1] Chemists, however, are normally constrained to use a sequence of several extremely time-consuming reactions for synthesis of these complex molecules, manipulating functional groups and forming covalent bonds one by one. Here we study near-equilibrium chemical systems where complex molecules are formed from simple fragments by symmetry-breaking steps and/or molecular growth processes. The relevant field is that of the polyoxometallates,^[2, 3] which exhibit not only unique topological and electronic versatility, with immense importance because of their wide range of application,^[2-4] but also the fascinating property that fragments can be linked, starting from simple units that resemble Platonic solids and progressing stepwise through the

mesoscopic range, where they appear in many forms, towards macroscopic compounds with network structures.^[2, 5, 6]

These and related aspects are demonstrated here through the study of the formation of two discrete molecular systems which are formed by basic conservative self-organization and growth processes and contain 37 and between 63 and 69 metal atoms, respectively.

Results and Discussion

The first of these is the cluster anion of the racemic reddish brown compound $(\text{NH}_4)_{14}[\text{H}_{14}\text{Mo}_{37}\text{O}_{112}] \cdot 35 \text{H}_2\text{O}$ (**1**) (Figures 1 and 2) which represents an unusual binary molecular species formed by a self-assembly process and which contains no symmetry element. The anion **1a** of the diamagnetic, mixed-valence compound **1** (type I according to the classification of Robin and Day^[7]) obtained from molybdate solution (see below), consists of a central $\{\text{H}_6\text{Mo}_{12}^{\text{V}}\text{O}_{40}(\text{Mo}^{\text{V}}\text{O}_3)_4\}$ core and two similar but non-identical coordinated ligands ($\{\text{Mo}_{10}\}$ and $\{\text{Mo}_{11}\}$, Figures 1 and 2). The ligands differ with respect to the number of Mo centres (10 or 11) and the degree of reduction and protonation. The core is built up from an $\{\text{Mo}_{12}^{\text{V}}\text{O}_{40}\}$ ϵ -Keggin type of subcore^[8] which is capped by four $\{\text{Mo}^{\text{V}}\text{O}_3\}$ groups. The $\{\text{Mo}_{11}\}$ ligand (Figure 1 bottom), which has approximately σ symmetry, is mainly built up of two incomplete Mo_3O_4 cubes with

[*] Prof. Dr. A. Müller, Dipl.-Chem. J. Meyer, E. Krickemeyer, Dipl.-Chem. C. Beugholt, Dr. H. Bögge, Dipl.-Chem. F. Peters, M. Schmidtman, Dipl.-Chem. P. Kögerler, M. J. Koop
Fakultät für Chemie der Universität Bielefeld
Lehrstuhl für Anorganische Chemie I
Postfach 100131, D-33501 Bielefeld (Germany)
Fax: (+49) 521 106-6003
E-mail: amueller@cheops.chemie.uni-bielefeld.de

octahedrally coordinated Mo atoms (Mo 18, Mo 23, Mo 24 and Mo 21, Mo 26, Mo 27, respectively). Two MoO_6 octahedra of the first Mo_3O_4 unit are connected through *edges* to the (neighbouring) MoO_6 octahedra (Mo 22, Mo 25) linking the two Mo_3O_4 units, while the third is bonded to an MoO_3 cap (Mo 14) of the central $\{\text{H}_6\text{Mo}_{12}^{\text{V}}\text{O}_{40}(\text{Mo}^{\text{VO}_3})_4\}$ core. All molybdenum atoms are of the Mo^{V} type and the $\mu_3\text{-O}$ and the three $\mu_2\text{-O}$ atom(s) are protonated. The three MoO_6 octahedra forming the second Mo_3O_4 unit are bonded to (neighbouring) polyhedra through *corners*. As this Mo_3O_4 unit contains exclusively Mo^{VI} centres, with only the $\mu_3\text{-O}$ atom being protonated, its formal charge is the same as that of the

first unit. The ligand contains one additional Mo^{V} centre (Mo 17) and interestingly is coordinated to five oxygen atoms forming an unusual square pyramid, which shares one edge with a second MoO_3 cap (Mo 13) of the central $\{\text{H}_6\text{Mo}_{12}^{\text{V}}\text{O}_{40}(\text{Mo}^{\text{VO}_3})_4\}$ core. Two further Mo^{VI} atoms (Mo 19 and Mo 20; the corresponding octahedra are linked through corners to those of the Mo 22 and Mo 25 atoms respectively) cap two Mo_3O_4 units of the central $\{\text{H}_6\text{Mo}_{12}^{\text{V}}\text{O}_{40}(\text{Mo}^{\text{VO}_3})_4\}$ core, thus completing Mo_4O_4 cubes. In the $\{\text{Mo}_{10}\}$ ligand, the two incomplete Mo_3O_4 cubes comprise the Mo 29, Mo 33, Mo 34 and Mo 31, Mo 36, Mo 37 atoms, respectively. One of the previously mentioned Mo^{VI} -type centres (the one corresponding to Mo 19 in the $\{\text{Mo}_{11}\}$ ligand) is missing, leaving one Mo_3O_4 unit of the $\{\text{H}_6\text{Mo}_{12}^{\text{V}}\text{O}_{40}(\text{Mo}^{\text{VO}_3})_4\}$ core uncapped and its three $\mu_2\text{-O}$ atoms protonated (Figure 1 top). Mo 32 and Mo 33 are in contrast with equivalent atoms (Mo 22, Mo 23) of the $\{\text{Mo}_{11}\}$ ligand of the Mo^{VI} type: Mo 32 has two terminal oxygen atoms (corresponding to the missing Mo atom) bonded to it and the two $\mu_2\text{-O}$ atoms of the Mo_3O_4 unit, bonded to Mo 33, are unprotonated.

The assignment of Mo^{V} and Mo^{VI} centres, as well as the protonation, clearly follows from bond-valence sum calcula-

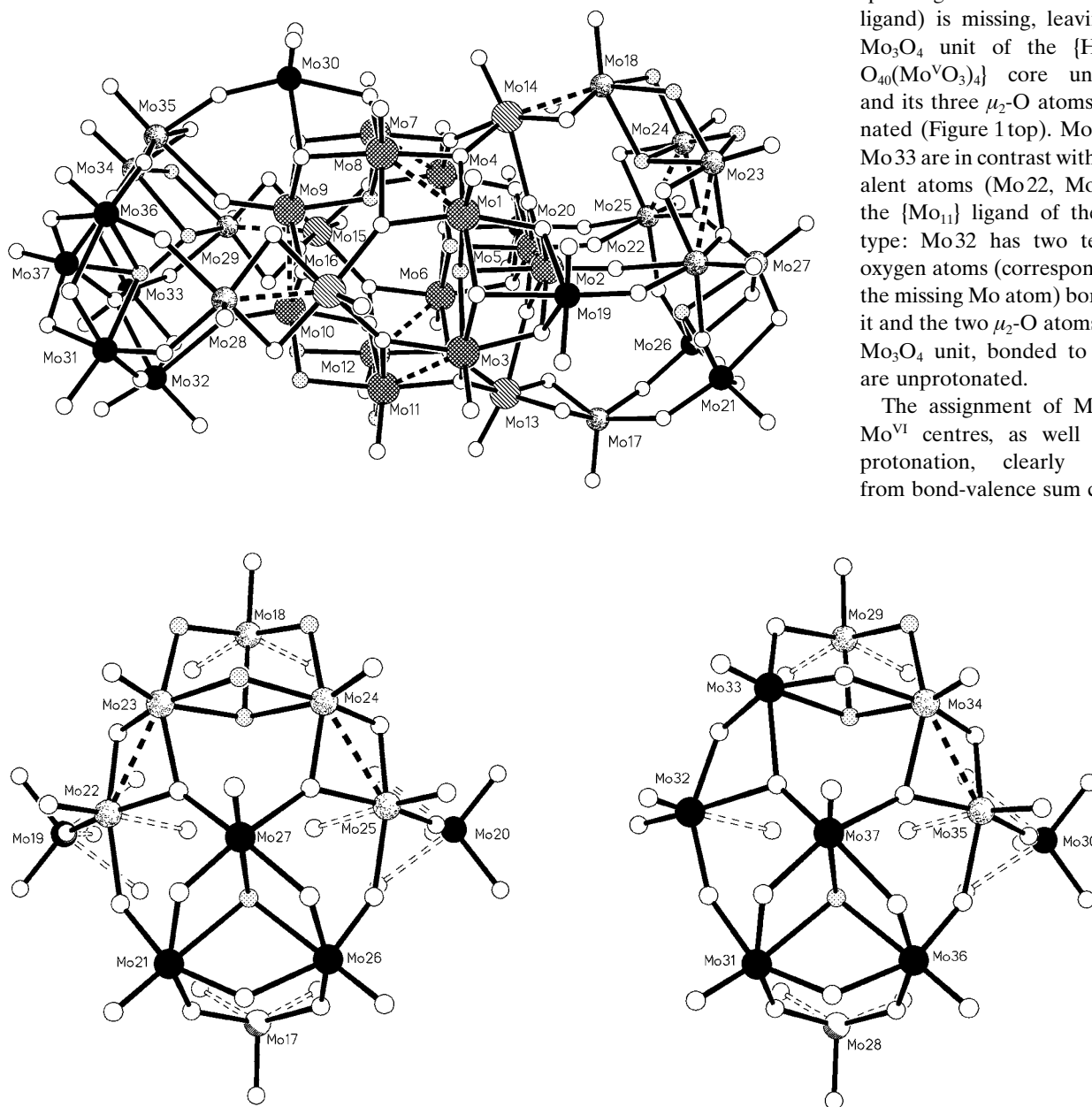


Figure 1: Top: Structure of the cluster anion of **1**. $\{\text{Mo}_{16}\}$ core: Mo atoms are enlarged (the 12 Mo atoms of the ϵ -Keggin core are cross-hatched and the four Mo atoms of the $\{\text{MoO}_3\}$ caps are hatched). $\{\text{Mo}_{10}\}$ and $\{\text{Mo}_{11}\}$ ligands: Mo^{V} centres are presented with a randomly dotted pattern and Mo^{VI} centres are black. All O atoms are shown as open circles, the OH groups are regularly dotted and the $\text{Mo}^{\text{V}}\text{-Mo}^{\text{V}}$ dumbbells are denoted by broken lines. Bottom: Structure of the $\{\text{Mo}_{11}\}$ (left) and $\{\text{Mo}_{10}\}$ ligands (right), and demonstration of their linking to the central $\{\text{Mo}_{16}\}$ core (represented by broken lines). The patterns of the relevant atoms are identical to those in Figure 1 top with the exception of the Mo centres (Mo 17, Mo 28) of the unusual MoO_5 square pyramids, which are white with dark shading.

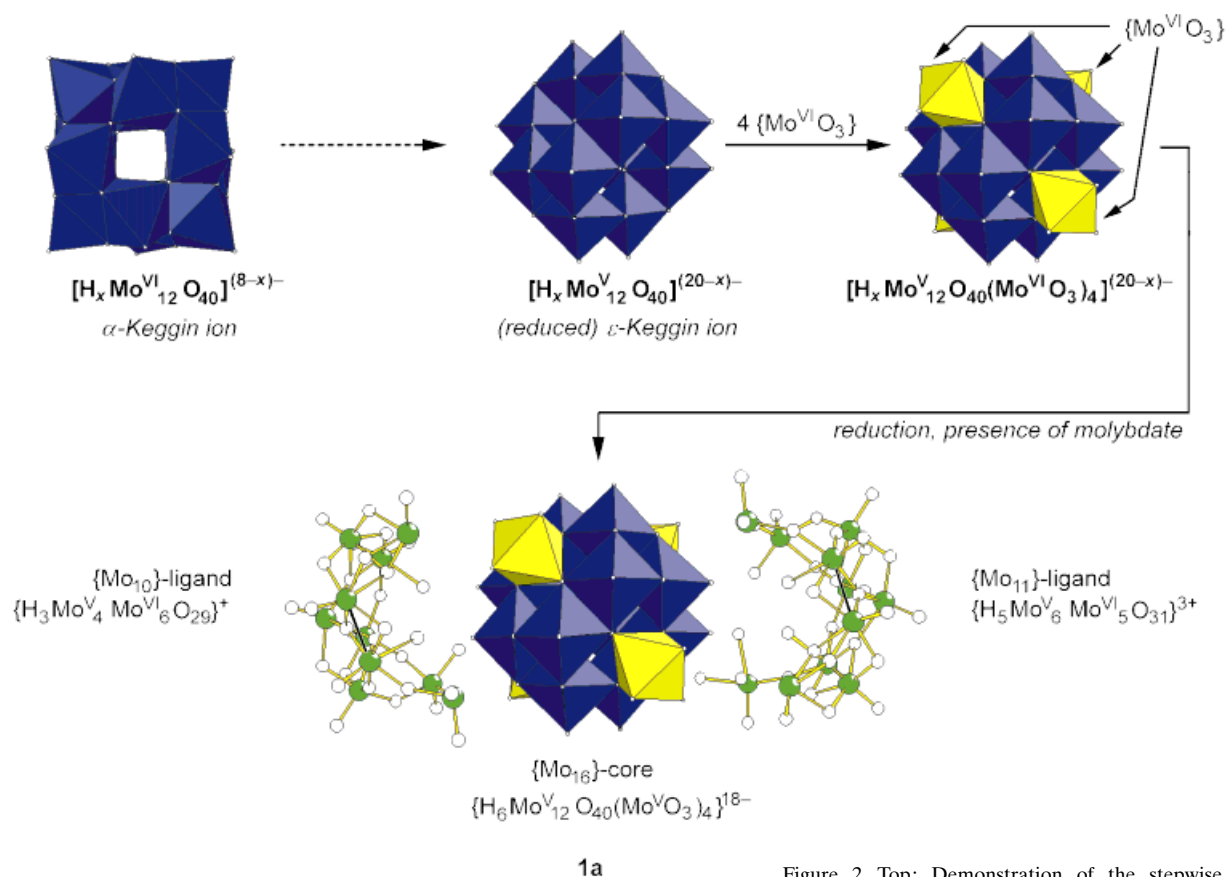


Figure 2. Top: Demonstration of the stepwise growth process leading to the cluster anion **1a** of **1**. The central highly nucleophilic ϵ -Keggin-type $\{H_x Mo_{12} O_{40}\}$ core and the four captured $\{MoO_3\}$ groups are shown as blue and yellow polyhedra, respectively. The $\{Mo_{10}\}$ - and $\{Mo_{11}\}$ -type ligands are represented as ball-and-stick models (Mo green; O white). Bottom: Reaction scheme corresponding to the growth process at the top of the Figure, demonstrating principally the step-by-step procedure in which nucleophiles attract electrophiles, which remarkably then become nucleophiles on the surface of the cluster upon reduction (see also text). O denotes species at the beginning of a growth process. $N_i(T)$ denotes a nucleophilic intermediate/fragment produced under reducing conditions ($2N-1$ according to Scheme 2) with a potential template function for the generation of the electrophilic intermediate E_i ($2n$, according to Scheme 2).

tions^[9] and is in agreement with the charge on the cluster corresponding to the number of cations and the fact that all Mo^V centres form the dumb-bell type of short (approx. 2.65 Å) $Mo-Mo$ bonds. This corresponds also to the brown colour, typical for systems with localized Mo^V-Mo^V pairs. In contrast with the low symmetry of **1a**, the related giant cluster anion $[Na(H_2O)_3 H_{13} Mo_3^V Mo_6^V O_{109} \{(OCH_2)_3 CCH_2 OH\}_7]^{7-}$ with a comparable central $\{Mo_{16} O_{52}\}$ core has (quite high) C_{3v} symmetry: its formation is controlled by the external organic pentaerythritol ligands.^[10]

The self-assembly of **1** takes place in aqueous molybdate solution under reducing conditions (in the presence of $N_2H_4 \cdot H_2SO_4$) and can be rationalized by assuming the initial formation of a cluster of the well-known α -Keggin type with T_d symmetry.^[11] Its reduction yields the highly nucleophilic ϵ -Keggin type cluster $[H_x Mo_{12} O_{40}]^{(20-x)-}$ (Figures 1 and 2).^[2, 8]

This species can be stabilized by protonation and by the capture of four electrophilic $\{Mo^VI O_3\}$ groups, thus forming an anion of the type $[H_x Mo_{12} O_{40} (Mo^VI O_3)_4]^{(20-x)-}$ which was isolated with a well-defined protonation, and has been structurally characterized as the $NH_2 Me_2^+$ salt.^[8] Remarkably, on further reduction ($Mo^VI \rightarrow Mo^V$) the originally electrophilic $\{Mo^VI O_3\}$ groups on the surface of the cluster themselves become nucleophilic and, in addition, assume a template function. In a type of synergistic co-assembly they evidently attract further electrophilic polyoxometallate fragments with 10 and 11 molybdenum atoms ($\{Mo_{10}\} \equiv [H_3 Mo_4^V Mo_6^VI O_{29}]^+$ and $\{Mo_{11}\} \equiv [H_5 Mo_6^V Mo_5^VI O_{31}]^{3+}$) the formation of which is due to the information stored in the $\{Mo_{16}\} (\equiv [H_6 Mo_{12}^V O_{40} (Mo^V O_3)_4]^{18-})$ nucleus or its template function (see Figure 2). Finally, the anion of **1** of the type $[\{Mo_{16}\} \{Mo_{10}\} \{Mo_{11}\}]^{14-}$ mentioned above is consequently

produced through a type of symmetry-breaking step (Figures 1 and 2). The asymmetric growth can be attributed in principle to the asymmetric protonation of only three of the four μ_3 -oxygen atoms forming the central cavity (see Figure 1); this may cause an asymmetric charge distribution and protonation on the surface of the intermediate (see also ref. [8]). In this context, it should be noted that self-assembly of very simple ingredients normally leads to products of high symmetry^[2, 12] (see also refs. [6, 13]).

In the case of large metal–oxygen clusters containing six vanadium and between 57 and 63 molybdenum centres, a novel type of molecular growth process takes place which can be considered to mimic specifics of an important class of transition metal oxides with relevance to materials science, especially to catalysis.^[14, 15] The cluster anion of the corresponding compound with the lowest Mo content, $(\text{NH}_4)_{21}[\text{H}_3\text{Mo}_{57}\text{V}_6(\text{NO})_6\text{O}_{183}(\text{H}_2\text{O})_{18}] \cdot 55\text{H}_2\text{O}$ (**2**)—its $\{\text{Mo}_{57}\text{V}_6\}$ centre comprising three large $\{\text{Mo}_{17}\}$ fragments linked by six V^{IV} centres and three $\{\text{Mo}_2\}$ -type entities—is

shown in Figure 3 (bottom, left).^[16, 17] An interesting structural feature is the presence of six rather large cavities located on the outer sphere between the $\{\text{Mo}_{17}\}$ fragments (Figure 3, bottom). These are accessible to the coordination of further highly electrophilic metal–oxygen fragments such as the $\{\text{MoO}\}^{4+}$ groups, thus resulting—in aqueous solution under specific experimental parameters (reducing conditions ($\text{NH}_2\text{OH} \cdot \text{HCl}$) and in the presence of an excess of molybdate which, according to the preparation method, is added to a solution containing **2a**)—in a step-by-step growth process which enables all species of the type $\{\text{Mo}_{57+x}\text{V}_6\}$ ($x = 0–6$) to be formed. Each of the $\{\text{MoO}\}^{4+}$ groups binds to three oxygen atoms (two terminal) of the $\{\text{Mo}_{57}\text{V}_6\}$ core of **2a**, resulting in a tetrahedral coordination of the incorporated Mo atoms. The degree of occupation of the cavities can be correlated with the degree of reduction of the cluster system. Reduction increases the nucleophilicity of the cluster periphery compared with **2a** and initiates a type of growth process in which up to as many as six electrophilic $\{\text{MoO}\}^{4+}$ entities—as

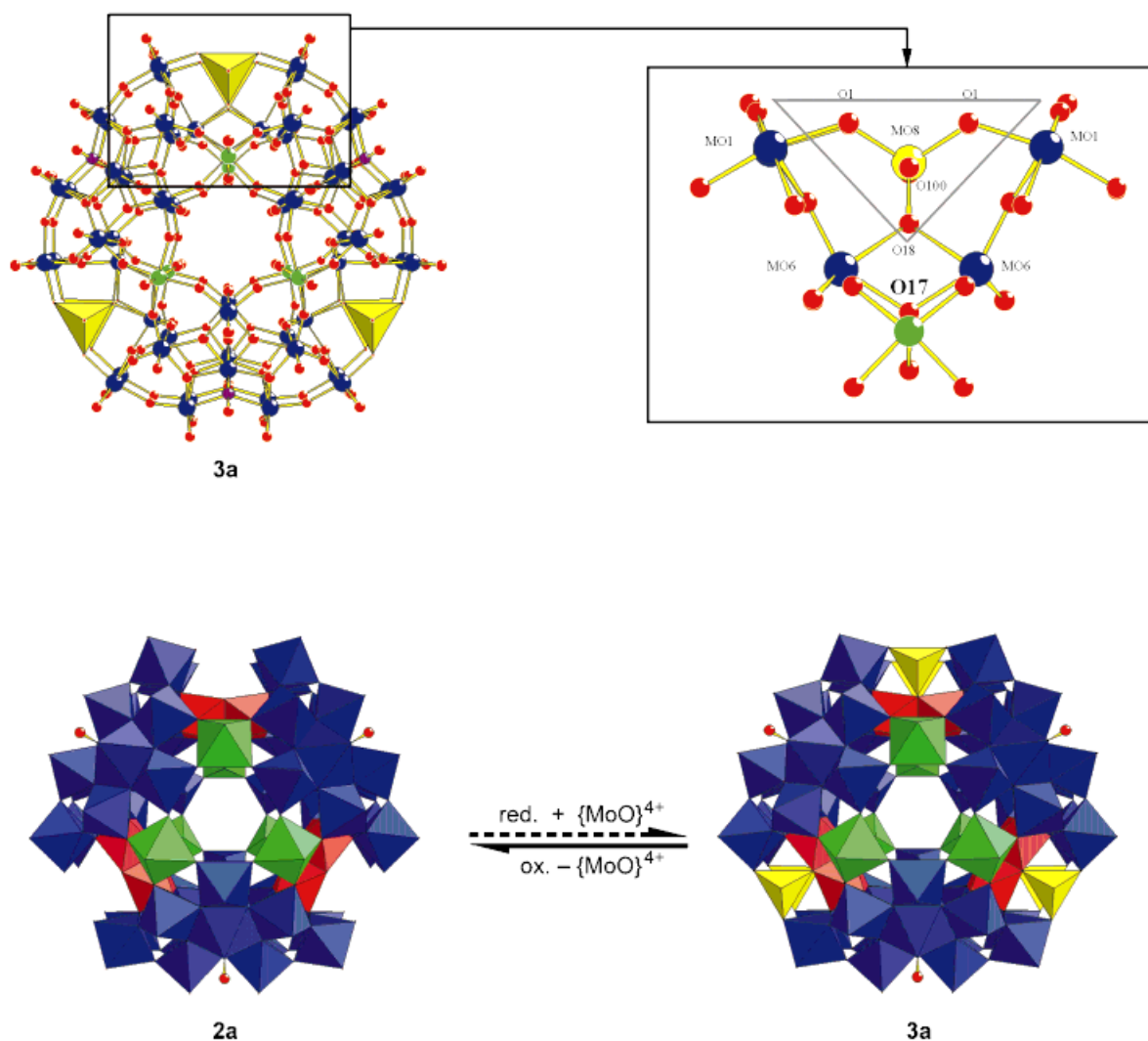


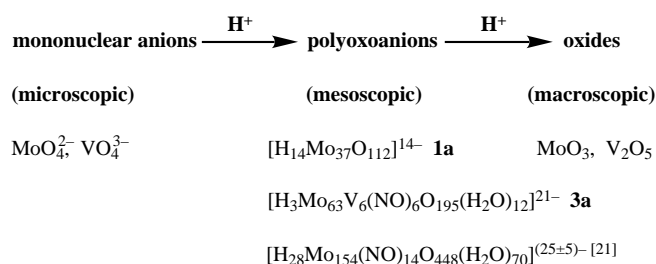
Figure 3. Top: Structure of the cluster anions **2a** and **3a** (Mo blue; V green; O red; N purple) showing extra MoO_4 tetrahedra (yellow polyhedral representation) together with one of the segments characteristic of the Uptake of $\{\text{MoO}\}^{4+}$ groups relative to **2a**. Bottom: Uptake (formal) and release of $\{\text{MoO}\}^{4+}$ groups in the case of the cluster anions of **2** and **3** (**2a** and **3a**, respectively) and of those with stoichiometries between these two. The central $\{\text{Mo}_{57}\text{V}_6\}$ core of each, **2a** and **3a**, is built up of three $\{\text{Mo}_{17}\}$ units (blue, polyhedral representation), which are linked by three $\{\text{Mo}_2\}$ entities (red) and six V^{IV} centres (green). The six $\{\text{MoO}\}^{4+}$ groups (including the relevant coordinating O atoms of **3a**) are represented as yellow tetrahedra.

in the case of the newly synthesized blackish blue compound $(\text{NH}_4)_{18}\text{Na}_3[\text{H}_3\text{Mo}_{57}\text{V}_6(\text{NO})_6\text{O}_{189}(\text{H}_2\text{O})_{12}(\text{MoO})_6] \cdot 41 \text{H}_2\text{O}$ (**3**)—can be incorporated. A formal increase in the positive charge on the corresponding cluster anion **3a** by each of the $\{\text{MoO}\}^{4+}$ groups is locally compensated since a twofold deprotonation of the bridging oxygen atom O18 together with the reduction of two symmetry-equivalent Mo 1 atoms in the direct vicinity can be observed (see Figure 3, top). Whereas high values (approx. 5.90) of the Mo bond-valence sums are found for the Mo1-type atoms ($\equiv \text{Mo}^{\text{VI}}$) on the periphery of the cluster anion **2a**, in the reduced species **3a**—a mixed-valence ($\text{Mo}^{\text{V}}/\text{Mo}^{\text{VI}}$) compound of type III according to the classification of Robin and Day^[7]—with 12 4d electrons (not considering the electronically isolated $\{\text{Mo}(\text{NO})\}^{3+}$ and the $\{\text{Mo}_2^{\text{V}}\}$ groups^[16]) the corresponding atoms show a much lower value (5.25). In **2**, six 4d electrons are almost localized in the above-mentioned $\{\text{Mo}_2^{\text{V}}\}$ units.^[16, 17]

The cavity mentioned above will now be described in detail. All the incorporated $\{\text{MoO}\}^{4+}$ groups (Mo 8; see Figure 3, top) which are located in the symmetry-equivalent cavities between the $\{\text{Mo}_{17}\}$ units are bound to three oxygen atoms also found in the parent anion **2a**.^[16] Two of these are the (formerly terminal) oxygen atoms (O1) of two neighbouring $\{\text{Mo}_{17}\}$ units of **2a**. The third atom (O18) is located on a crystallographic mirror plane and connects two Mo atoms (Mo6) of the $\{\text{Mo}_2^{\text{V}}\}$ unit (see Figure 3, top, and refs. [16, 17]). This oxygen atom is doubly protonated in **2a** and here, owing to coordination to the $\{\text{MoO}\}^{4+}$ group, it is (formally) deprotonated. Furthermore, standard extended Hückel calculations correspondingly reveal the LUMO in **2** to be mostly localized on peripheral positions close to the vacant cavities.

Interestingly, the (formal) uptake of electrophilic $\{\text{MoO}\}^{4+}$ groups is reversible upon oxidation (Figure 3b). Indeed, the entire process can be regarded as a model for biological metal assembly processes that are dependent on electron transfer, or metal centre uptake and release in metal storage proteins; for instance this model is valid for ferritin with more than 4000 Fe atoms^[18] or for the Mo storage protein of the N_2 -fixing microorganism *Azotobacter vinelandii* with approximately 16 Mo atoms organized in a polyoxomolybdate unit.^[19] The tetranuclear Mn complex in the photosystem II of green plants, for example, is formed by the stepwise binding of four Mn^{II} centres accompanied by photooxidation to produce Mn^{III} .^[18] In the ferritin case, growth of the metalcentre core occurs by oxidative processes on the surface of the mineral type particle.

In general, polyoxometallates represent a class of polynuclear, anionic metal–oxygen clusters with an extraordinary topological and overwhelming structural variety in the mesoscopic region, which lies between simple, mononuclear species such as MoO_4^{2-} or VO_3^{3-} and compounds with typical solid-state structures and which is characterized by a quasi-infinite number of possible arrangements of linked building units.^[5, 12, 20] Their ability to develop from the molecular world and to gradually approach that of macroscopic structures predestines the polyoxometallates for the study of phenomena relating to stepwise self-organization (as in the cases mentioned above) of nanoscale material systems with the concomitant generation of complexity (Scheme 1).



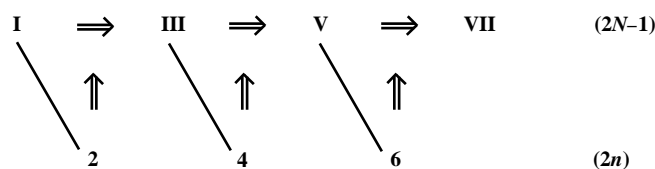
Scheme 1. Stepwise self-organization of polymetallates.

In the examples mentioned above, growth or self-assembly processes lead to highly complex structures; thus the molecular complexity increases (generally with a concomitant decrease in symmetry^[22, 23]) with increasing numbers of elements, of relevant interlinkages and of different types of linkages.

A prerequisite for molecular growth in the case of polymolybdates such as **1** and **2** is the facile reducibility of the starting material and/or the relevant intermediates in the reaction mixture. The reduction results in an increase in nucleophilicity on certain regions of the cluster periphery and a subsequent capture of (further) electrophilic entities in a specific manner. The highly negatively charged species, such as those in Figure 2, remain intact in solution because of the large repulsive interactions between them and the protection against hydrolysis whereby the large enthalpy of hydration allows the continuation of a growth process.

In the biological world, the overall generation of complexity occurs under dissipative conditions (that is, far from equilibrium), and with simultaneous entropy export. Complex biomolecules, for example, or even bioclusters, are produced stepwise by several gene-directed processes. The FeMo cofactor of the FeMo-protein nitrogenase for instance—an unusual hetero metal–sulfur cluster important for the development and existence of life on Earth—is generated stepwise with the help of various genes.^[24]

In this context, however, we also have to address the basic question of whether it is possible to create molecular complexity, not only far from equilibrium as in the biosphere, but also under near-equilibrium conditions, by some conservative growth process (Scheme 2) including feedback



Scheme 2. Conservative growth process with feedback reactions.

reactions, if the ingredients are selected correspondingly. The odd capital Roman numerals $2N-1$ represent steps of a growing molecular system and the even lower-case Arabic numerals $2n$ stand for ingredients in the solution which react only with one particular product. Each intermediate $2N-1$, such as the $\{\text{Mo}_{16}\}$ nucleus in the case of **1a** or the $\{\text{Mo}_{57}\text{V}_6(\text{Mo})_x\}$ ($x=0-5$) cores of the species finally leading

to **3a**, carries information (in J. Monod's sense) for the formation of the subsequent intermediate $2n$, such as $\{\text{Mo}_{10}\}$, $\{\text{Mo}_{11}\}$ and $[\text{MoO}]^{4+}$, respectively, which was not originally abundant in solution. The complex system at the end of the growth process is generated by a symmetry-breaking step (see also ref. [25]). It should be stressed, however, that during the growth process in the case of **1a** the decrease in symmetry from T_d to C_1 cannot be attributed to the same type of symmetry breaking as that of more usual first- and second-order phase transitions, for instance during crystallization from solution or during transformation from paramagnetism to ferromagnetism. In these cases, symmetry breaking refers to the whole system.^[22, 23]

Complex, giant, electron-rich metal oxide cluster anions obtainable in this way may have multifunctional properties: a high density of states in the HOMO/LUMO region with pseudo-band structure and a narrow band gap (prerequisites for small molecular semiconductors), electron-storage properties and thus potential suitability as redox catalysts,^[2] tunable magnetic exchange interactions according to a stepwise substitution of paramagnetic centres (a prerequisite for the generation of different types of molecular magnets),^[26–28] the capability for growth, nanoscale cavities and corresponding host properties.^[21] Furthermore, their large surface areas model those of solids, such as mixed-valence transition metal oxides with catalytic activity.^[14]

The important conclusion is that systems or intermediates containing building blocks with fairly high free energy (here, species with populated antibonding orbitals upon reduction), which can be linked in different ways under different conditions, can generate in a stepwise manner a huge variety of species with high molecular complexity (this is also valid for amino acids, of course; see, for example, refs. [29, 30]). The route leading to the end product, according to Scheme 2, might include feedback reactions and reaction pathways involving several intermediates ($2N - 1$) of the molecular system, in growth with a possible template function for the formation of intermediates ($2n$) reacting with the relevant $2N - 1$ species. This type of reaction is not only relevant for prebiotic processes, but concerns the generation of complex material systems in general.

Experimental Section

Synthesis and spectroscopic data of $(\text{NH}_4)_{14}[\text{H}_{14}\text{Mo}_{37}\text{O}_{112}] \cdot 35\text{H}_2\text{O}$ (1**):** $(\text{NH}_4)_6[\text{Mo}_7\text{O}_{24}] \cdot 4\text{H}_2\text{O}$ (14 g, 11.3 mmol), NH_4Cl (14 g, 261.9 mmol) and $\text{N}_2\text{H}_4 \cdot \text{H}_2\text{SO}_4$ (2 g, 15.4 mmol) were dissolved in a mixture of water (350 mL) and 100% acetic acid (1.5 mL) and heated to 100 °C (color change, blue to green to brown). After keeping the solution for 2 h at this temperature, the resulting brown precipitate was filtered off from the hot solution, then the filtrate was cooled to 20 °C and allowed to stand for 1–2 weeks in an Erlenmeyer flask covered with a watchglass. The brown crystalline fraction of **1** was separated from a fine brown precipitate by repeated suspension of the latter in the filtered mother liquid

followed by decantation. Yield: 5.6 g (42% relative to Mo). $\text{H}_{140}\text{Mo}_{37}\text{N}_{14}\text{O}_{147}$: calcd H 2.24, Mo 56.90, N 3.14; found H 2.15, Mo 56.1, N 3.12; IR (KBr pellet): $\tilde{\nu} = 1615$ (m, $\delta(\text{H}_2\text{O})$), 1400 (s, $\delta_{\text{as}}(\text{NH}_4^+)$), 960 (s), 905 (s) ($\tilde{\nu}(\text{Mo}=\text{O})$); 865 (m), 780 (vs), 745 (vs), 600 (m), 505 cm^{-1} (m); UV/Vis (solid-state reflectance spectrum): $\lambda = 390$ nm (br).

Synthesis and spectroscopic data of $(\text{NH}_4)_{21}[\text{H}_3\text{Mo}_{57}\text{V}_6(\text{NO})_6\text{O}_{183}(\text{H}_2\text{O})_{18}] \cdot 55\text{H}_2\text{O}$ (2**):** An improved method was followed:^[16] a mixture of $(\text{NH}_4)_6[\text{Mo}_7\text{O}_{24}] \cdot 4\text{H}_2\text{O}$ (8.7 g, 7.0 mmol), $\text{NH}_2\text{OH} \cdot \text{HCl}$ (4 g, 57.5 mmol), NH_4Cl (4.6 g, 86.0 mmol) and H_2O (150 mL) was heated in a 300 mL wide-necked Erlenmeyer flask covered with a watchglass at 60 °C without stirring for 17 h. The hot solution was filtered and stored at room temperature. The precipitated red crystals of $(\text{NH}_4)_{12}[\text{Mo}_{36}(\text{NO})_4\text{O}_{108}(\text{H}_2\text{O})_{16}] \cdot 33\text{H}_2\text{O}$ (**4**) (see ref. [16]) were filtered off after 6 h (yield: 91%). Compound **4** (2 g, 0.312 mmol) was added to a 0.5 M aqueous VOCl_2 solution (22 mL) which was subsequently heated at 90 °C for 30 min. After a brownish precipitate had been filtered from the hot solution, NH_4Cl (0.5 g) was added to the purple filtrate, which was then stored at room temperature for crystallization; violet hexagonal crystals of **2** were deposited within three days. Yield: 0.79 g (36% relative to Mo). $\text{H}_{233}\text{Mo}_{57}\text{N}_{27}\text{O}_{262}\text{V}_6$: calcd H 2.21, Mo 51.69, N 3.57, V 2.89; found H 1.7, Mo 51.52, N 3.52, V 2.76.

Synthesis and spectroscopic data of $(\text{NH}_4)_{18}\text{Na}_3[\text{H}_3\text{Mo}_{57}\text{V}_6(\text{NO})_6\text{O}_{189}(\text{H}_2\text{O})_{12}(\text{MoO}_6)] \cdot 41\text{H}_2\text{O}$ (3**):** Aqueous solutions of $\text{Na}_2\text{MoO}_4 \cdot 2\text{H}_2\text{O}$ (14.92 g, 61.7 mmol, in 100 mL), NH_4VO_3 (2.38 g, 20.3 mmol, heated in 200 mL) and $\text{NH}_2\text{OH} \cdot \text{HCl}$ (25.66 g, 369 mmol, in 100 mL) were combined in a 500 mL round-bottomed flask (with formation of a yellow precipitate) and acidified with 3.5% hydrochloric acid (9.5 mL). The flask was covered with a watchglass and heated for 6 h without stirring in an oil bath (105 °C) (color changes: initially yellow, to orange, to greenish brown, to dark blue). The resulting dark blue precipitate was filtered off from the hot solution and the filtrate refluxed for about 20 min under an argon atmosphere. After it had been cooled to approximately 80 °C, $\text{Na}_2\text{MoO}_4 \cdot 2\text{H}_2\text{O}$ (20 g, 82.7 mmol) was added. The mixture was refluxed again for 20 min and

Table 1. Crystal data, data collection and refinement parameters.

	1	2	3 ^[a]
sum formula	$\text{H}_{140}\text{Mo}_{37}\text{N}_{14}\text{O}_{147}$	$\text{H}_{233}\text{Mo}_{57}\text{N}_{27}\text{O}_{262}\text{V}_6$	$\text{H}_{181}\text{Mo}_{63}\text{N}_{24}\text{Na}_3\text{O}_{254}\text{V}_6$
M_r	6239.04	10579.35	11001.50
color	brown	violet	blue
crystal dimensions [mm]	$0.4 \times 0.1 \times 0.06$	$0.4 \times 0.3 \times 0.3$	$0.2 \times 0.08 \times 0.08$
crystal system	monoclinic	hexagonal	hexagonal
space group	$C2/c$	$P6_3/mmc$	$P6_3/mmc$
T [K]	203	183	203
a [Å]	27.173(5)	23.496(1)	23.587(7)
b [Å]	44.085(11)	23.496(1)	23.587(7)
c [Å]	23.427(9)	26.811(1)	26.542(12)
α [°]	90	90	90
β [°]	103.49(2)	90	90
γ [°]	90	120	120
V [Å ³]	27289(13)	12818.1(9)	12788(8)
Z	8	2	2
ρ_{calcd} [g cm ⁻³]	3.04	2.74	2.86
$\mu(\text{Mo}_{\text{K}\alpha})$ [mm ⁻¹]	3.40	3.02	3.31
$2\theta_{\text{max, measured}}$ [°]	47	54	50
reflections measured	22498	72170	8532
unique reflections (R_{int})	19996	5110	4181
observed ($I > 2\sigma(I)$)	13728	4304	2434
refined parameters	994	295	304
$R_1^{\text{[b]}}$ ($F_o > 4\sigma(F_o)$)	0.0814	0.0485	0.067
$wR_2^{\text{[c]}}$	0.190	0.122	0.181
$\Delta\rho(\text{max/min})$ [e Å ⁻³]	2.4/−1.4	1.78/−1.19	1.53/−2.14

[a] Several other structures of compounds of the type $\{\text{Mo}_{57+x}\text{V}_6\}$ which contain between 57 and 63 Mo atoms were determined but are not listed here. The corresponding disorder problems with respect to different occupied positions of clusters in different unit cells will also not be discussed here. This refers also to different possible sites for the three protons in case of **3** though these are clearly found in the bridging O atoms of the $\{\text{Mo}_3\}$ groups of **2**.^[16, 17]

$$[\text{b}] R_1 = \frac{\sum |F_o| - |F_c|}{\sum |F_o|}, [\text{c}] wR_2 = \sqrt{\frac{\sum w(F_o^2 - F_c^2)^2}{\sum w(F_o^2)^2}} \text{ with } 1/w = \sigma^2(F_o^2) + \frac{0.1(F_o^2 + 2F_c^2)}{3}$$

subsequently slowly cooled to room temperature. From the dark blue mother liquor which was stored at 5 °C for crystallization under an argon atmosphere, black, needle-shaped, air-sensitive crystals were precipitated within 5–7 days. They were separated by filtration and dried in an argon stream. Under similar but less reducing conditions and without subsequent addition of Na₂MoO₄·2H₂O, intermediates between **2** and **3** of formula {Mo_{57+x}V₆} (with x = 1–5) were formed. Yield: 2.0 g (18.6% relative to Mo). H₁₈₁Mo₆₃N₂₄Na₃O₂₅₄V₆: calcd H 1.66, Mo 54.94, N 3.06, Na 0.63, V 2.78; found H 1.7, Mo 55.10, N 2.93, Na 0.60, V 2.70; IR (KBr pellet): $\tilde{\nu}$ = 1580 (s, δ (H₂O)), 1400 (s, δ_{as} (NH₄⁺)), 970 (m, ν (V=O)), 890 (s, ν (Mo=O)), 805 (vs), 765 (s), 670 (s), 575 (s), 545 cm⁻¹ (s); (resonance) Raman (degassed H₂O/HCl; pH 1.4, λ_c = 1064 nm): $\tilde{\nu}$ = 953 (w), 883 (m), 826 (s), 451 cm⁻¹ (m); UV/Vis (degassed H₂O/HCl; pH 1.4): λ = 741 nm (ϵ_{mol} = 6.1 × 10⁴ L mol⁻¹ cm⁻¹; IVCT); the ϵ value can be related to the number of Mo^V centers even in case of decomposition.

Single crystal X-ray structure analyses: The measurements (MoK α radiation, graphite monochromator) were carried out with a Siemens three-circle diffractometer with a 1K-CCD detector (1272 frames each of which covering 0.3° in ω , for **2**) and with a Siemens four-circle diffractometer (Wyckhoff scans for **1** and **3**). Lorentz and empirical absorption corrections were applied. All structures were solved with direct methods using the program SHELXS-96^[31] and refined against F^2 by full-matrix least-squares using the program SHELXL-93.^[32] The sites of reduced metal centres as well as the protonated O atoms were determined by bond-valence sum calculations.^[9] Further details of the crystal structure determination reported in Table 1 may be obtained from the Fachinformationszentrum Karlsruhe, D-76344 Eggenstein-Leopoldshafen (Germany), on quoting the depository numbers CSD 407984 for **1**, CSD 407986 for **2** and CSD 407985 for **3**.

Acknowledgements: We thank the Deutsche Forschungsgemeinschaft and the Fonds der Chemischen Industrie for financial support.

Received: July 29, 1997 [F784]

- [1] F. Cramer, *Chaos and Order*, VCH, Weinheim, **1993**, p. 37.
- [2] M. T. Pope, A. Müller, *Angew. Chem.* **1991**, *103*, 56–70; *Angew. Chem. Int. Ed. Engl.* **1991**, *30*, 34–48.
- [3] *From Platonic Solids to Anti-Retroviral Activity*, (Eds.: M. T. Pope, A. Müller), Kluwer, Dordrecht, **1994**.
- [4] Y. Izumi, K. Urabe, M. Onaka, *Zeolite, Clay, and Heteropoly Acids in Organic Reactions*, VCH, Weinheim, **1993**.
- [5] A. Müller, *Nature (London)* **1991**, *352*, 115.
- [6] A. Müller, H. Reuter, S. Dillinger, *Angew. Chem.* **1995**, *107*, 2505–2539; *Angew. Chem. Int. Ed. Engl.* **1995**, *34*, 2328–2361.
- [7] M. B. Robin, P. Day, *Adv. Inorg. Chem. Radiochem.* **1967**, *10*, 247–422.
- [8] M. I. Khan, A. Müller, S. Dillinger, H. Bögge, Q. Chen, J. Zubieta, *Angew. Chem.* **1993**, *105*, 1811–1814; *Angew. Chem. Int. Ed. Engl.* **1993**, *32*, 1780–1782; A. Müller, S. Dillinger, E. Krickemeyer, H. Bögge, W. Plass, A. Stammler, R. C. Haushalter, *Z. Naturforsch. B.* **1997**, *52*, 1301–1306.
- [9] a) I. D. Brown in *Structure and Bonding in Crystals, Vol. II* (Eds.: M. O'Keeffe, A. Navrotsky), Academic Press, New York, **1981**, pp. 1–30; b) N. E. Breese, M. O'Keeffe, *Acta Crystallogr. Sect. B* **1991**, *47*, 192–197.
- [10] M. I. Khan, Q. Chen, J. Salta, C. J. O'Connor, J. Zubieta, *Inorg. Chem.* **1996**, *35*, 1880–1901.
- [11] J. F. Keggin, *Nature (London)* **1933**, *131*, 908–909.
- [12] A. Müller, C. Beugholt, *Nature (London)* **1996**, *383*, 296–297.
- [13] A. Müller, E. Krickemeyer, S. Dillinger, H. Bögge, A. Stammler, *J. Chem. Soc. Chem. Commun.* **1994**, 2539–2540.
- [14] V. E. Henrich, P. A. Cox, *The Surface Science of Metal Oxides*, Cambridge University Press, Cambridge, **1996**.
- [15] C. Schlenker, *Low-Dimensional Electronic Properties of Molybdenum Bronzes and Oxides—Physics and Chemistry of Materials with Low-Dimensional Structures, Vol. 12*, Kluwer, Dordrecht, **1989**.
- [16] A. Müller, E. Krickemeyer, S. Dillinger, H. Bögge, W. Plass, A. Proust, L. Dloczik, C. Menke, J. Meyer, R. Rohlfing, *Z. Anorg. Allg. Chem.* **1994**, *620*, 599–619.
- [17] A. Müller, W. Plass, E. Krickemeyer, S. Dillinger, H. Bögge, A. Armatage, A. Proust, C. Beugholt, U. Bergmann, *Angew. Chem.* **1994**, *106*, 897–899; *Angew. Chem. Int. Ed. Engl.* **1994**, *33*, 849–851.
- [18] R. P. Hausinger in *Mechanisms of Metallocenter Assembly: Advances in Inorganic Chemistry* (Eds.: R. P. Hausinger, G. L. Eichhorn, L. G. Marzilli), VCH, Weinheim, **1996**, pp. 1–18.
- [19] a) P. T. Pienkos, W. J. Brill, *J. Bacteriol.* **1981**, *145*, 743–751; b) A. Müller, W. Suer, C. Pohlmann, K. Schneider, W.-G. Thies, H. Appel, *Eur. J. Biochem.* **1997**, *246*, 311–319.
- [20] J.-P. Jolivet, M. Henry, J. Livage, *De la Solution à l'Oxyde*, Inter Editions/CNRS Editions, Paris, **1994**.
- [21] A. Müller, E. Krickemeyer, J. Meyer, H. Bögge, F. Peters, W. Plass, E. Diemann, S. Dillinger, F. Nonnenbruch, M. Randerath, C. Menke, *Angew. Chem.* **1995**, *107*, 2293–2295; *Angew. Chem. Int. Ed. Engl.* **1995**, *34*, 2122–2124.
- [22] H. Haken, *Synergetics—Nonequilibrium Phase Transition and Self-Organization in Physics, Chemistry and Biology*, Springer, Berlin, **1977**.
- [23] T. Mayer-Kuckuk, *Der gebrochene Spiegel—Symmetrie, Symmetriebrechung und Ordnung in der Natur*, Birkhäuser, Basel, **1989**.
- [24] A. Müller, E. Krahn, *Angew. Chem.* **1995**, *107*, 1172–1179; *Angew. Chem. Int. Ed. Engl.* **1995**, *34*, 1071–1078.
- [25] A. Müller, K. Mainzer in *From Simplicity to Complexity in Chemistry—and Beyond* (Eds.: A. Müller, A. Dress, F. Vögtle), Vieweg, Wiesbaden, **1996**, pp. 1–11 and other chapters.
- [26] D. Gatteschi, L. Pardi, A. L. Barra, A. Müller, J. Döring, *Nature (London)* **1991**, *354*, 463–465.
- [27] A. L. Barra, D. Gatteschi, L. Pardi, A. Müller, J. Döring, *J. Am. Chem. Soc.* **1992**, *114*, 8509–8514; A. Müller, W. Plass, E. Krickemeyer, R. Sessoli, D. Gatteschi, J. Meyer, H. Bögge, M. Kröckel, A. X. Trautwein, *Inorg. Chim. Acta* **1998**, *271*, 9–12.
- [28] D. Gatteschi, A. Caneschi, L. Pardi, R. Sessoli in *From Simplicity to Complexity in Chemistry—and Beyond* (Eds.: A. Müller, A. Dress, F. Vögtle), Vieweg, Wiesbaden, **1996**, pp. 171–192.
- [29] J. P. Ferris, A. R. Hill Jr, R. Liu, L. E. Orgel, *Nature (London)* **1996**, *381*, 59–61.
- [30] G. von Kiedrowski, *Nature (London)* **1996**, *381*, 20–21.
- [31] G. M. Sheldrick, SHELXS-96, University of Göttingen, **1996**.
- [32] G. M. Sheldrick, SHELXL-93, University of Göttingen, **1993**.